THE DESIGN AND CONSTRUCTION OF A MASS SPECTROGRAPH

by

KEITH A. MORE

B. S., Kansas State College of Agriculture and Applied Science, 1951

A THESIS

submitted in partial fulfillment of the
requirements for the degree

MASTER OF SCIENCE

Department of Physics

KANSAS STATE COLLEGE
OF AGRICULTURE AND APPLIED SCIENCE

1953

TABLE OF CONTENTS

INTRODUCTION

The realization of relatively accurate determinations of the masses of atoms has been accomplished by the use of the mass spectrograph. The mass spectrograph development dates back as far as 1897 when J. J. Thomson (7) performed his now classical experiment to determine the charge to mass ratio of the electron. Later, in 1910, Thomson modified his apparatus to measure the charge to mass ratio of a singly charged atom. The first element analyzed was neon of average atomic weight 20.2 which was shown to consist of two isotopes of atomic mass numbers 20 and 22. Since then many modifications in design have been made so that the modern spectrograph is an instrument of precision. Some of the latest models (1, 5) have resolving powers such that detection of mass differences of one part in 10,000 are possible.

There are four major fields of application for which the mass spectrograph is now used. These fields employ the mass spectrograph or a mass spectrometer* for accurate isotope mass determination, for analysis of chemical mixtures by identification of isotopic masses, to determine relative abundances of different isotopes, and to separate isotopes of a given element in quantity.

Spectrographs designed for accurate isotope mass determinations emphasize high resolving power, with the consequent reduction of large quantity separation. On the other hand, spectrographs used for quantity

* The mass spectrometer differs from the mass spectrograph only in the collection and detection of the isotopes. The mass spectrograph uses a photographic plate detector while the spectrometer employs some sensitive electrical means for detection of the isotope.

separation relax the high resolving power. When used for analysis, both high resolving power and large quantity separation are de-emphasized in the interests of simplicity and versatility.

The purpose for which the instrument described below was constructed was two-fold: as a tool for isotope analysis mainly in the rare-earth region, and as a small quantity separator of radioactive materials. These requirements demanded an instrument somewhat between that of an analytical and a precision type spectrograph.

The description of the instrument together with its design and construction features are discussed in the section entitled Design and Construction. To explain the choice of design, some of the essential theory of the mass spectrograph is first presented in the following section entitled Theory of the Mass Spectrograph.

THEORY OF THE MASS SPECTROGRAPH

General Theory

The basic principle underlying the operation of a mass spectrograph is the action of a magnetic field on a moving charged particle.

A particle of mass M, velocity v and charge e, when projected into a uniform magnetic field of strength B, describes a circular trajectory of radius R, according to the well-known formula, equation 1.

1. $$\frac{Mv^2}{R} = \frac{Bev}{10}$$

By a simple manipulation this formula reduces to equation 2.

2. $$R = \frac{\sqrt{2ME10^2}}{Be}$$

Here, E, equal to $1/2\ Mv^2$, is the kinetic energy of the particle.

The mass spectrograph employs an electrostatic field to give a group of ions an energy E. When this ion beam is directed into a uniform magnetic field the ions of different masses describe circular arcs of different radii of curvature, and thus may be separated from each other.

To express the radii of curvature in terms of measurable quantities, the kinetic energy E may be replaced by the work done on the ion by the electric field V, according to equation 3.

3. $$E = \tfrac{1}{2}Mv^2 = Ve10^7$$

Equations 2 and 3 then yield the following formula:

4. $$R = \frac{\sqrt{2MV10^9}}{Bve} = K M; \quad K = \frac{\sqrt{2V \cdot 10^9}}{Bve}$$

The quantity K is a constant for any one separation.

In these equations, masses are in grams, distances in centimeters, velocities in centimeters per second, charge in coulombs, magnetic field in gausses, and potential in practical volts.

In principle a well collimated beam of ions is directed into a magnetic field where the various isotopes are separated into a mass spectrum and collected upon a photographic plate. However, it is evident that collection of ions in reasonable quantity requires some relaxing of the degree of collimation of the ion beam. In general, divergence of the ion beam gives rise to a finite 'line width' on the photographic plate in place of the infinitesimal width indicated by equation 4. Kerwin and Geoffrin (3) have shown that the line width may be minimized by proper design of the instrument. Part of the following discussion is taken from their work.

Magnetic Focussing

Figure 1 shows an ideal focussing situation, which may be explained as follows: A is the source of accelerated ions which is directed into the magnetic field. The contour POP' defines the shape of the pole faces. As shown below, proper shaping of this contour will allow focussing of the ion beam at the point B irrespective of the emission angle θ.

Assuming a symmetric contour about the line OY, so that OA is equal to OB, the proper shape for focussing at the point B may be deduced. Employing the terminology of Fig. 1 it is seen that

$$5. \qquad \tan\theta = \frac{Y}{a-x} = \frac{x}{\sqrt{R^2-x^2}}$$

where R is given by equation 4. Thus the field contour OP is given by

$$6. \qquad y = \frac{x(a-x)}{\sqrt{R^2-x^2}}$$

Deviations from this ideal focussing condition arise mainly from two sources: the fringing effects on the magnetic field at the pole face periphery, and the finite extent of the source, as opposed to the point source assumed in the derivation.

In practice it is common to collimate the beam and use a portion of this periphery. In the interests of easier pole face construction the curved surface is usually replaced by a straight line contour, tangent to the ideal contour and passing through O as in Fig. 2. The central portion of the beam, at angle θ, is then directed perpendicularly to the tangent line. It is seen that the source, center of curvature and the focal point must lie along the same straight line.

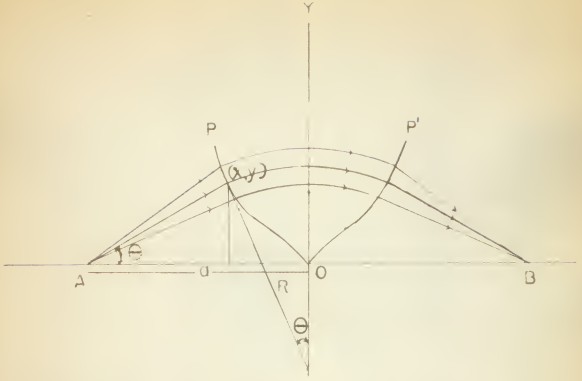

Fig. 1. Contour of pole face for perfect focussing

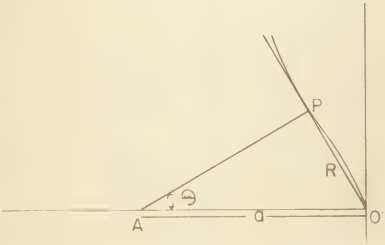

Fig. 2. Straight line approximation to perfect focussing field contour

The foregoing discussion considers only the symmetric focussing of ions of a single mass. When different masses are present in the same beam it is clear that only approximate focussing will be obtained. Particles of heavier mass will approximately focus at points to the right of B, while those of lighter mass will focus to the left of B.

The dependence of the approximate focal position on the photographic plate with respect to the mass of the isotope is a function of the central angle θ. As will be shown, the widely used choice of θ equal to 30 degrees leads to a simple dependence.

Plate I shows the simplified arrangement frequently employed for mass spectrographs. The essential theoretical feature that the source A, focal plane (x axis), and the center of the 60 degree pole faces are coplanar, is retained.

As remarked earlier isotopes of different masses will focus at different points along the focal plane. The following derivation of the correlation between mass numbers and focussing positions employ the following terminology partially illustrated in Plate I.

M_0 Mass of symetrically focussed particle;

R_0 Radius of curvature of particle of mass M_0;

x_0 Focussing position on x axis for particle of mass M_0;

η Distance along OP' between the paths of particle of mass M and particle of mass M_0 as they leave the magnetic field;

θ The difference in angle between the arcs of paths of M and M_0;

R The radius of curvature of particle of mass M;

L The distance from field edge to x axis along a path parallel to path of M_0 particle, and at a distance η away from M_0 path;

EXPLANATION OF PLATE I

Diagram of 60° Sector Magnetic Field

The parameters shown in the diagram are used in the derivation of equation 13.

PLATE I

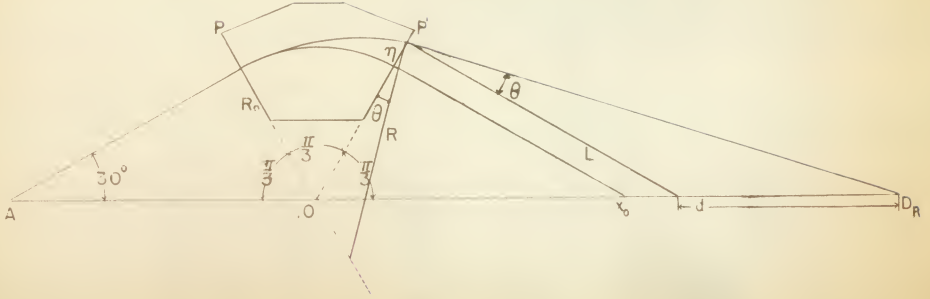

d The distance along the x axis between the terminus of L and the path of particle of mass M;

D_r The position along the x axis at which the particle of mass M strikes;

From Plate I and by the use of the law of sines it is seen that:

7. $x_o = R_o/\sin 30 = 2R_o$

8. $L = (2R_o + 2\eta)\sin 60 = (R_o + \eta)\sqrt{3}$

9. $\frac{d}{\sin\theta} = \frac{L}{\sin(\pi - 150 - \theta)} = \frac{\sqrt{3}(R_o + \eta)}{\sin(30 - \theta)}$

10. $\frac{R}{\sin 60} = \frac{R_o + \eta}{\sin(60 - \theta)} = \frac{R - R_o}{\sin\theta}$

11. $D_r = x_o + 2\eta + d = 2R_o + 2\eta + \sqrt{3}(R + \eta)\frac{\sin\theta}{\sin(30 - \theta)}$

Substituting relation 10 for $R_o + \eta$ and by using trigonometric identies, equation 11 reduces to equation 12.

12. $D_R = (R - R_o)\frac{\sqrt{3}\cot^2\theta - \cot\theta}{\cot\theta - \sqrt{3}}$

It is convenient to parameterize these relations by absorbing the variable R in the demensionless ratio $\beta = R_o/R$.

For small θ, the sin θ may be replaced by tan θ . With this substitution the approximate relation, equation 13, follows:

13. $D_r = 2\frac{R_o + R}{3\beta - 1} = 2R_o\frac{(1 + 1/\beta)}{3\beta - 1}$

The validity of this approximation can be seen from Fig. 3. in which exact computations of D_R/R are compared with the approximate relation, equation 13. The dispersion $\frac{\Delta D}{\Delta M}$ may be calculated as follows, employing the approximate relation 13:

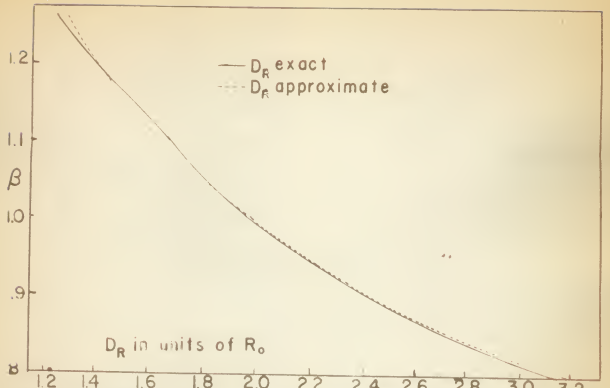

Fig. 3. Correlation curve of versus D_R for exact and approximate values.

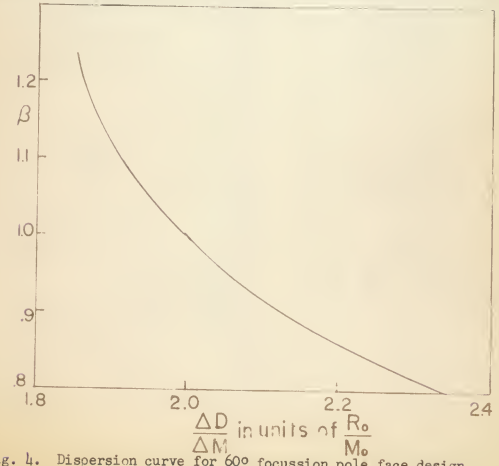

Fig. 4. Dispersion curve for 60° focussion pole face design.

$$\frac{\Delta D}{\Delta M} = \frac{\Delta D}{\Delta R}\,\frac{\Delta R}{\Delta M}$$

$$R = K\sqrt{M} = \frac{R_o}{\sqrt{M_o}}\sqrt{M}$$

$$\frac{\Delta R}{\Delta M} = \frac{R_o}{\sqrt{M_o}}\,\frac{1}{2\sqrt{M}} = \frac{R_o^2}{2M_oR} = \frac{R_o}{2M_o}\beta$$

$$\frac{\Delta D}{\Delta R} = \frac{(3R_o-R)\,(2R_o+4R) + 2R(R_o+R)}{(3R_o-R)^2} = 2\left[\frac{12}{(3-1/\beta)^2} - 1\right]$$

thus

$$14.\quad \frac{\Delta D}{\Delta M} = \frac{R_o\beta}{R_o}\left[\frac{12}{(3-1/\beta)^2} - 1\right]$$

A parameterized plot of $\Delta D/\Delta M$ versus β is shown in Fig. 4.

Line Broadening

The basic design of the instrument has been governed largely by the theoretical considerations given in the previous subsection on Magnetic Focussing. These design features include the general shape of the pole faces, the location of the ion source and the photographic plate detector.

To keep the Design and Construction section of this report relatively free of justifications many of the arguments governing particular choices of design and instrumentation are presented here.

Most of the finer details of construction can be related to efforts to make the most of the resolution permitted by the preceeding theory. A number of factors all tend to give a broadened image on the detector, in place of the idealized discrete lines.

First, a natural or geometrical broadening of the image arises from several factors. These include us of a source of finite width and height, failure to employ pole faces designed for perfect focussing and employing the instrument to detect ions far removed from the symmetrically focussed ions. To minimize these effects, narrow sources and collimated beams were used, while the electric and magnetic fields were adjusted to position the spectra under separation about the point x_0.

The finite source length caused line broadening in the following manner. Equation 4 assumed a monoenergetic beam with the momentum of each ion directed perpendicularly to the magnetic field. However, Fig. 5 shows that due to the finite extent of the source, the pole gap and the detector in the direction of the field, some ions will be focussed which have momentum components parallel to the field.

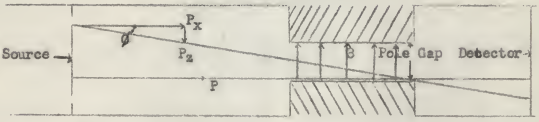

Fig. 5. Diagram of the line broadening, due to finite source length.

If the beam is monoenergetic the forward momentum will be less for the ion leaving at an angle ϕ as compared to an ion for which ϕ is zero. To determine the magnitude of line broadening from this effect substitute $\frac{P^2}{2M}$ for E in equation 4 and take the logarithmic derivative. This gives equation 15.

15. $\frac{\Delta R}{R} = \frac{\Delta P}{P}$.

The variation of R from this cause was kept to within a few parts out of 10,000 by the use of a short filament and narrow pole gap.

Line broadening which was not geometric in nature was manifested in the following ways; collision with gas particles, thermal energy spread of the positive ions, and variation of the electric and magnetic field.

The collision of ions with gas particles results in the scattering of the ion beam. To minimize this effect all portions of the ion path were evacuated. A discussion of the vacuum system is given in the section on Design and Construction.

Line broadening also results from the variable thermal energy received by the ions. In any ionizing process energy is supplied to an atom which drives off an electron leaving the atom as a positively charged ion. In order to obtain an abundant supply of positive ions more energy than is required to ionize the atom must be supplied. This leaves ions in a group with a small spread of thermal energies. To estimate the magnitude of this effect, as well as some others to be mentioned, consider equation 16, obtained by logarithmically differentiating equation 2.

16. $$\frac{\Delta R}{R} = \frac{\Delta E}{E} - \frac{\Delta B}{B}$$

The variation of potential over the source required for heating was maintained at only a fraction of a volt whereas the accelerating potentials were of the order of thousands of volts. This reduced the thermal line broadening to only a few hundredths of a percent. The use

of high accelerating voltage also minimizes effects of air scattering of the beam. However, it is seen from equation 16 that variations of either the magnetic field or the potential field would result in line broadening. To reduce these effects both of these fields were regulated.

Several other sources of line broadening include possible reflections of ions from camera components, mutual Coulomb repulsion of ions in the beam, fringing effects of the magnetic field, and possible space charge effects at the source end.

The camera has been designed to keep the ion path as free as possible from obstructing members. Reference to Plate II shows that after passing the collimating slits, the point at which ions enter the magnetic field offers the main source of reflections. Lewis and Hayden (4) have indicated that gold plated slits keep reflection effects to a minimum. Consequently the defining slits at this point were gold plated.

No evidence has been found that space charging at the source or Coulomb repulsion of the beam is significant. Presumably, at high enough beam currents these effects might be serious.

An accurate analysis of the fringing effect on the focussing of the beam has not been carried out. However, the fringing field does have the effect of extending the effective magnetic field somewhat past the periphery of the pole pieces. Nier (6) allows for this effect by assuming an extension of the field over the periphery by a distance equal to the thickness of the pole gap. This approximation was also employed here. Consequently, the plane containing the source and the detector is offset from the geometric center of the pole pieces to allow for the fringing field.

DESIGN AND CONSTRUCTION

General Description of the Instrument

A careful survey of the literature was made before a particular design was chosen. The instrument employed by Lewis and Hayden (4) in their research on radioactive isotopes contained most of the desired features of an analytic and small quantity separator mass spectrograph. Plate II shows details of the spectrographic camera and ion source described here, which with a few modifications, is essentially that of Lewis and Hayden.

The following brief description of the operation of the instrument can best be understood by referring to Plate II.

Ions were driven off the heated filament C, maintained at a high positive potential. They then passed through the defining slit E and continued on through the brass tube H, which provided the ion path to the magnet. The particles were accelerated to high energy during their passage from C to E, since slit E was held at nearly ground potential. On entering the magnetic field the beam was again collimated by a gold-plated slit.

Isotopes of different masses were then separated by the action of the magnetic field established by the pole pieces I. The separated isotope beams then continued through the camera J, and were deposited on the photographic plate L.

Plate III gives a photograph of the complete mass spectrograph. The electronic apparatus was mounted on a portable rack and the spectrograph was built upon a movable wooden stand. This made the entire

EXPLANATION OF PLATE II

Construction Diagram of Mass Spectrograph

A - To Ammeter

B - To High Voltage

C - Tungsten Filament

D - To Filament Transformer

E - Defining Slit

F - Pyrex Glass Spacer

G - Sylphon Bellows

H - Brass Tube

I - Nier Type Pole Pieces

J - Brass Box

K - 1/4 inch brass spacers with a 3/32 inch diameter magnetic field probe hole

L - Photographic Plate

M - Thermocouple Vacuum Gauge

N - Ion Source Holder

P - Phosphor-bronze spring with lucite insulation, which secures ion source holder, N, in place.

PLATE II

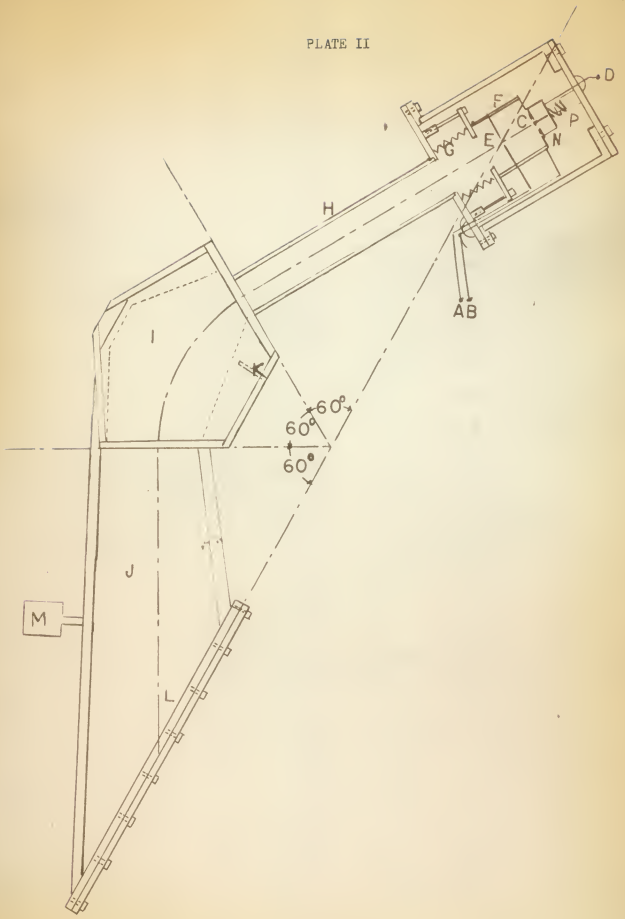

EXPLANATION OF PLATE III

Photograph of Complete Mass Spectrograph

At the left is the electronic apparatus rack. From top to bottom:

Scaling unit supplying high accelerating voltage;

Vacuum ion gauge control:

Vacuum tube voltmeter;

Magnet power supply;

Current regulator with accompanying battery packs.

At the right is the mass spectrograph stand showing the following components:

The magnetic pole pieces and exciting coils;

The camera assembly;

The Western Electric D79512 ion gauge tube at the top of the instrument;

The two diffusion pumps with their water cooling system.

The filament control panel is at bottom left, the thermocouple gauge control is at the bottom center. The switches at bottom right control the diffusion pumps and the fore-pump. The fore-pump can be seen in the rear.

PLATE III

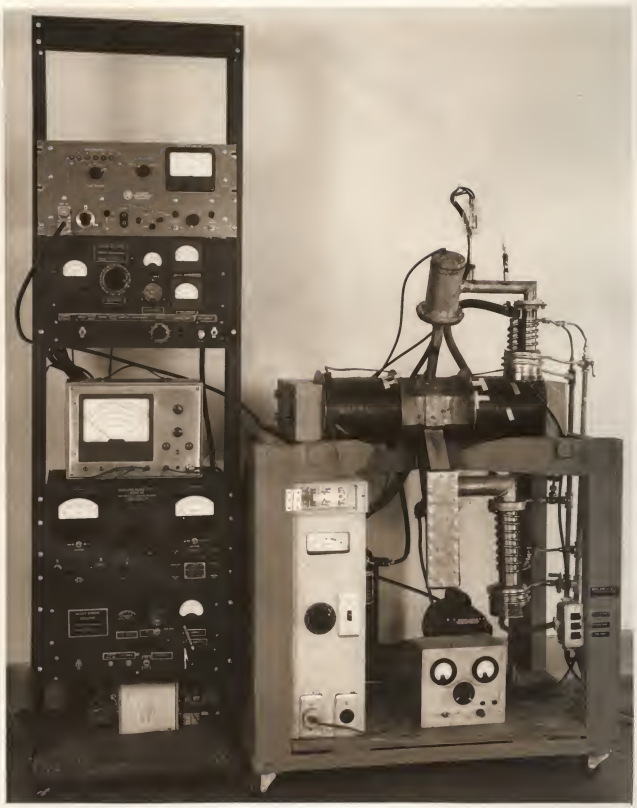

apparatus portable. A discussion of the various components follows under the subtitles The Ion Source, The Magnetic Field, The Detector and The Vacuum System.

The Ion Source

The thermal emission of positive ions from a heated filament was employed. Blewett and Jones (2) reported very efficient yields of single charged positive ions of the alkaline earths as well as from Sr, Ba, Y, Ce and from a few other elements. Lewis and Hayden (4) extended the list to include many elements in the rare-earth region.

A diagram of the filament holder and ion accelerator are shown on Plate IV. Photographs of the ion source holder and ion accelerator are given in Fig. 2 and Fig. 3 of Plate IV. The relations of these components to the complete spectrograph can be seen on Plates II, III, and V.

The ion source holder was made of nichrome. Nichrome plate, D, 1/4 inch by 5/8 inch with a centered slit 1/16 inch by 1/2 inch was spot-welded to a rectangular cylinder of nichrome, as shown on Plate IV, Fig. 1. Centered in this slit was a tungsten filament .005 inch by .030 inch in cross-section and 7/16 inch long on which the source was deposited. The ends of the filament were spot-welded to two nichrome wires of 22 B&S gauge. One wire was soldered to the holder and the other wire was soldered to a Kovar seal.

The ion accelerator consisted of two nichrome discs, C and D of Fig. 1, Plate IV, each 1-1/4 inch in diameter. These were separated by a pyrex spacer, F, 25 mm in diameter and 1 cm long. Disc C had a

EXPLANATION OF PLATE IV

Fig. 1 Diagram of ion source holder and ion accelerator (Actual Size)

A - Kovar seal with nichrome wire to tungsten filament
B - Rectangular nichrome cylinder 1 inch long
C - Nichrome disc with slot for centering plate D
D - Nichrome plate which has a slot with tungsten filament centered in it
E - Nichrome plate with defining slit
F - Pyrex glass spacer
G - Pyrex glass spacer
H - Alignment screws
I - Sylphon bellows
J - Kovar seal with nichrome wire from defining slit E which goes to ammeter
K - Kovar seal with nichrome wire from slit C which goes to high accelerating voltage
L - Brass tube connecting ion source to magnet which houses ion beam.

Fig. 2 Photograph of ion source holders showing different degrees of construction.

From left to right: finished holder with lucite insulator and phosphor bronze spring attached; holder with filament soldered in place and Kovar seal with copper wire to battery snap; nichrome rectangular cylinder holder with 1/4 inch by 5/8 inch nichrome plate spot-welded to it.

Fig. 3 Photograph of ion accelerator.

PLATE IV

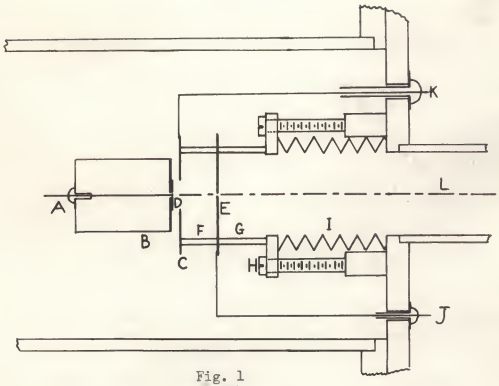

Fig. 1

Fig. 2

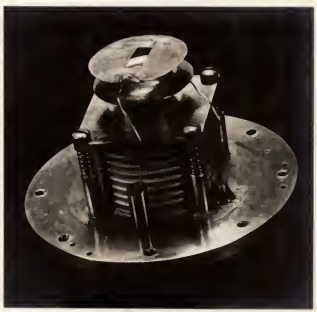

Fig. 3

EXPLANATION OF PLATE V

Schematic Diagram of Electrical, Water and Vacuum Connections to Mass Spectrograph

A - Water Drain

B - Water Input

C - Desicatting Flask containing Dryite

D - Mechanical Fore-pump

E - 110 volt AC Input

F - Three-stage MCF60 oil Diffusion Pump

G - Two-stage VMF10-W oil Diffusion Pump

H - Magnet Power Supply, 500 volts at 500 ma well-regulated

I - Magnet Current Regulator

J - Variac 200B

K - 5 volt Secondary Filament Transformer with 10,000 volt insulation

L - Ammeter showing Filament current

M - High-voltage Accelerating Potential Supply

N - Ammeter and Ion Gauge Control

O - Western Electric D79512 Ion Gauge

P - Outlet for connection to McLeod Gauge

PLATE V

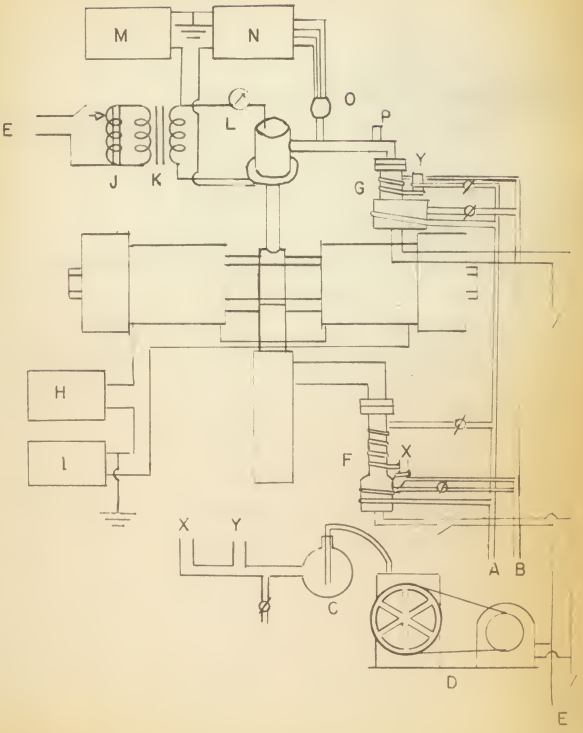

slit 1/4 inch by 5/8 inch in which the plate of the source holder was centered. Disc E had a slit .010 inch wide by .250 inch long and served to collimate the beam. The ion accelerator assembly was mounted on another pyrex spacer G, 25 mm in diameter and 1/2 inch long, which in turn was mounted on a square brass plate. All glass to metal joints were made with Armstrong A-6 adhesive. To enable adjustment of the direction of the ion beam a Sylphon bellows, I, was soldered between the ion accelerator assembly and the brass tube ,L, as shown in Plate IV, Fig. 1. Brass screws, H, were mounted in each of the four corners of the square brass plate to allow for alignment adjustments.

The combined ion source holder and ion accelerator assembly was covered with a brass cylinder which was terminated with a brass port as shown in Plate II. It was through this port that the source holder was removed to change samples. The holder was held securely in place by a lucite insulated, phosphor-bronze spring as shown in Fig. 2, Plate IV, and 'P' of Plate II.

The source holder and its adjoining disc C were at a high positive accelerating potential. This potential was obtained from a scaling circuit power supply regulated against line voltage variation to .001 per cent. The defining slit disc E was not grounded directly but passed in series with an ammeter to ground. This permitted a method of adjusting the ion beam since the beam current was proportional to the current collected on the defining slit disc. The filament current was supplied by a 5 volt filament transformer whose primary was connected to the secondary of a Variac 200B (Plate V). The secondary of the filament trans-

former had high voltage insulation. One side of the secondary was connected to the high voltage of the ion accelerator. The other side of the secondary was passed through a Kovar seal in the port of the ion source cover. Internal connection was made to the filament by means of battery snaps.

In preliminary tests of the ion source two methods of bonding the sample to the filament were used. In both cases barium was the test element. In one method a water solution of barium nitrate was deposited on the tungsten and dried. The other method employed a mixture of barium carbonate and collodian thinned with amyl acetate. This mixture was brushed onto the filament and dried with a heat lamp. Both methods proved successful, giving copious emission of ions.

When an accelerating voltage of 1600 volts was used it was found necessary to pass approximately seven amperes through the filament for several minutes before emission of ions could be obtained. The current could then be reduced to approximately four amperes for an ion current of one microampere. This phenomena has been explained by Blewett and Jones (2). They reported that it is first necessary to activate the source by intensive heating. This activation results in a deposit of a film of metallic barium and barium oxide on the surface of the filament. Once this film is formed ion currents can be drawn with considerably lower temperatures.

The ion current depended strongly on the magnitude of the accelerating voltage. For example, even with a filament current of 10 amperes an ion beam of only .2 microampere could be obtained with no accelerating voltage.

The ammeter used to measure plate currents serves a dual role and its discussion is given in the subsection on The Vacuum System.

The Magnetic Field

The magnet was constructed of Armco iron. The pole pieces (Plate VII, Fig. 1) were hexagonal and were from a design developed by Nier (6). A circle of 12.3 cm in diameter was inscribed in a hexagon in such a way that the two sides which lay along the 60° sector were each 9.4 cm long. Each pole piece was 3-1/2 inches thick and was nickel-plated to prevent corrosion. The two surfaces of each pole piece were ground parallel. As shown in Plate II, the pole faces were made an integral part of the camera assembly. To insure parallelity of the pole faces, 1/4 inch brass spacer bars, labeled 'K' in Plate II, were placed between the poles. The assembly of the pole face to the brass housing was made in the following manner: a pole face was bolted in its position and then soldered in place; the excess solder was wiped away and the brass spacers inserted and soldered in place. Then the other pole piece was inserted and checked for alignment with a micrometer and soldered in place. Micrometer measurements of the final assembly failed to reveal any deviations from uniformity of the pole gap. A photograph of this assembly is shown in Fig. 1, Plate VI.

It was found necessary to silver-solder the brass housing to prevent opening seams while soft-soldering to the pole pieces. Care had to be exercised in the soldering operation so as not to overheat the Armco iron and thus introduce magnetic nonhomogeneities. A 3/32 inch

EXPLANATION OF PLATE VI

Fig. 1 - Photograph of Mass Spectrograph with ion source cover removed. Hole in pole piece is tapped for 7/8 inch x 14 threads per inch stud to enable fastening to magnet.

Fig. 2 - Photograph of plate holder showing hinged clamp to hold photographic plate or film.

Fig. 3 - Photograph of Mass Spectrograph mounted on portable wooden stand.

PLATE VI

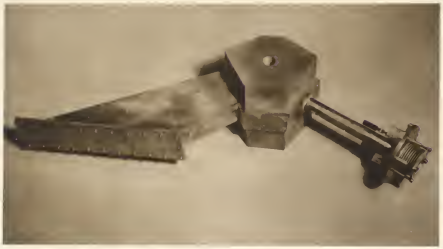

Fig. 1

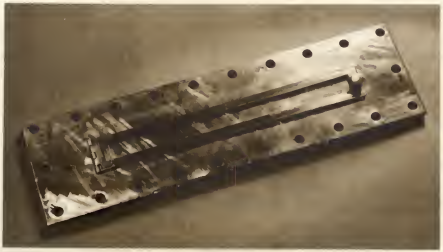

Fig. 2

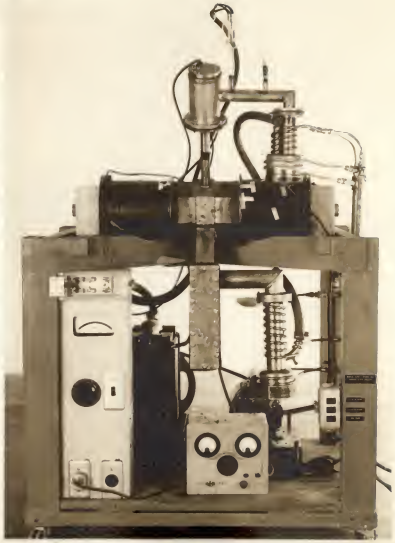

Fig. 3

EXPLANATION OF PLATE VII

Fig. 1 - Diagram of Nier-type Pole Face

Fig. 2 - Diagram of Magnet

PLATE VII

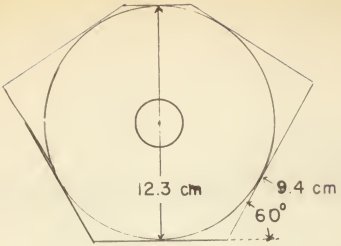

Fig 1

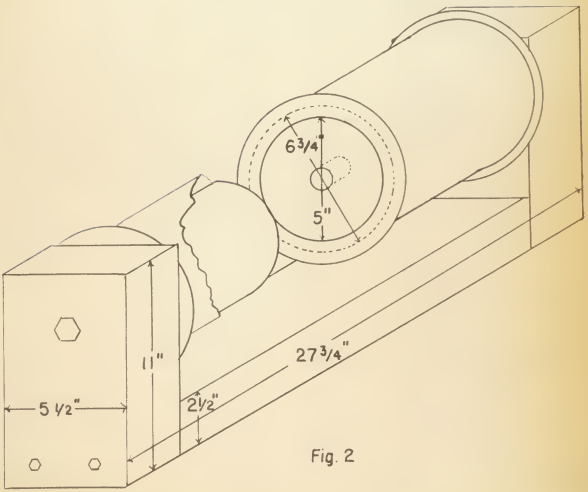

Fig. 2

hole was drilled into the brass spacer 1 inch deep, permitting insertion of the probe of a gaussmeter for approximate field measurements.

The Armco iron magnet was of conventional design as shown on Plate VII, Fig. 2. Studs made of Armco iron were used to bolt the coil cores to the pole pieces. Each coil had 12,000 turns of No. 24 Formvar-coated copper wire and had a resistance of 400 ohms. The coils were connected in series and energized by a regulated power supply of 500 volts. The negative terminal of the coil was connected to the current regulator as shown on Plate V. No excessive heating was observed at currents as high as one-half ampere.

Figure 6 presents a hysteresis curve for a magnetic field of 5,000 gausses maximum. Since less than a third of the maximum current available was used, it would appear from Fig. 6 that fields as high as 10,000 gausses should be obtainable. No provision for field measurements in excess of 5,000 gausses were readily obtainable.

The magnet current regulator, whose schematic is shown on Plate VIII, was a modification of the one used by Lewis and Hayden (4). It kept constant the current through the magnet coils by regulating the voltage developed by the current across a standard manganin resistor. Small voltage changes across the standard resistor were amplified by the three 6AK5's and the resultant voltage change was placed on the grids of the triode connected 6V6's in such a way as to counteract the voltage change across the manganin resistor. The power supply of the 6AK5's was of conventional design. To maintain the 6V6's operating on

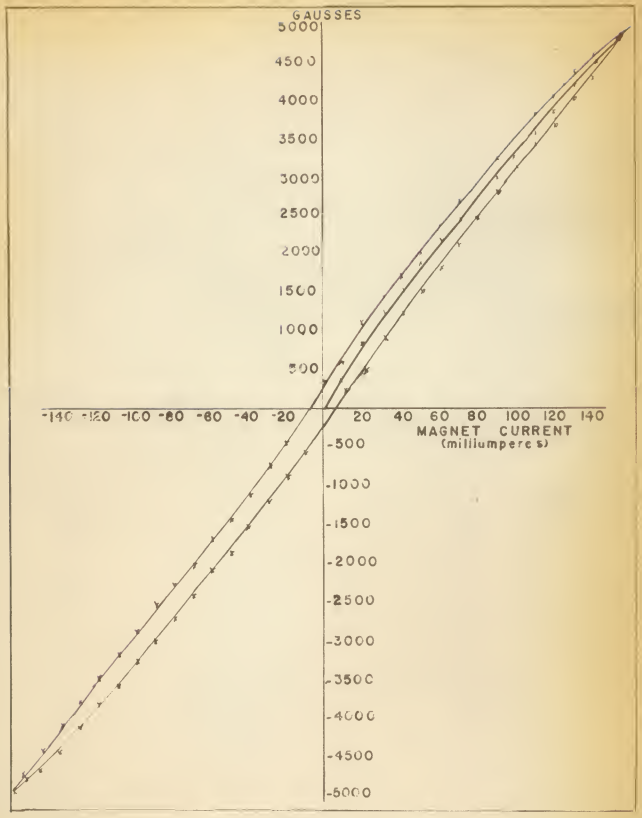

Fig. 6. Hysteresis Curve of Armco Iron Magnet

EXPLANATION OF PLATE VIII

Schematic Diagram of Magnet Current Regulator

Values of Circuit Elements

Tubes:

V1 thru V3 - 6AK5
V4 thru V23 - 6V6
V24, V25, V26 - 6B4
V27 - 12SJ7
V28 - 83

Batteries:

Ba 1 - 45v tapped every 3v
Ba 2 - 135 v
Ba 3 - 67½ v
Ba 4 - 22½ v

Switches:

S1 - DPST
S2 - DPDT
S3 - DP 3 position
S4 - SP 16 position
S5 - 9P 4 position

Transformer and Choke:

T1 - 117 volt pri. sec. 768V,CT, 150ma 6.3V, 5 amp.,5V, 3 amp.
L1 - 5 mh @ 350 ma

Meters:

M1 - Vacuum Tube Voltmeter
M2 - 0 - 10 ma
M3 - 0 - 1 ma

Capacitances:

C1, C2 - .1 microfarad
C3, C4 - 20 microfarads,450v.

Resistors:

R1 - 33K*
R2 - 0.5M**w.w.
R3 - 60 K**w.w.
R4 - 20K**w.w.
R5 - 10K**w.w.
R6 - 20K**w.w.
R7 - 1 M ***
R8 - 2.2 M***
R9 - 2.2 M***
R10 - 0.33 M***
R11 - 15 K* 1W
R12 - 4.7 K* 1W
R13 - 6.8 K* 1W
R14 thru R34 - 1 K*
R35 - 50** w.w.
R36 - 30** w.w.
R37 - 10** w.w.
R38 - 10** w.w.
R39 - 0.5 M***
R40 - 10K* w.w.
R41 - 300** w.w. 1W
R42 - 100**Manganin 4W
R43 - 30**Manganin 4W
R44 - 8**Manganin 4W
R45 - 1.2 K* w.w. 4W
R46 - 400** Manganin 4W
R47 - 120**Manganin 8W
R48 - 32** Manganin 8W
R49 - 680** w.w. 20W
R50 - 1 M*** w.w.

NOTE:
*K = 1,000 ohms
** = ohms
*** M = 1,000,000 ohms

PLATE VIII

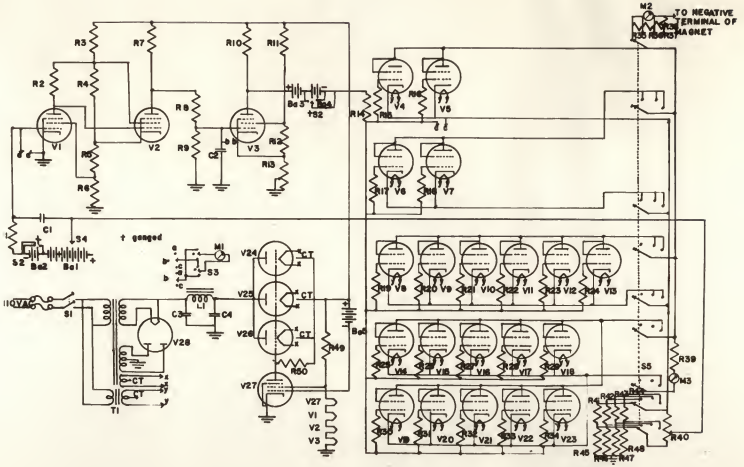
TO NEGATIVE TERMINAL OF MAGNET
R3
R7
R10
R11
R2
R4
R8
R9
R12
R13
R5
R6
V1
V2
V3
C2
Be3
Be4
R14
R15
V4
V5
R17
V6
R16
V7
C1
S4
S2
Be2
Be1
S3
M1
115VAC
S1
T1
V24
V25
V26
V27
C3
C4
R49
R50
Be5
V27
V1
V2
V3
V8
V9
V10
V11
V12
V13
V14
V15
V16
V17
V18
V19
V20
V21
V22
V23
R39
S5
M3
R40
R45
R46
R47
R48
M2
R38

a favorable part of their characteristic curves at low currents and not overload at high currents a gang switch connected or disconnected 6V6's in parallel. This same switch changed the meter range and manganin resistor.

The current was adjusted by changing the grid bias on the 6AK5 tubes V1 and V3. To obtain settings favorable to the 6AK5's tube characteristics provision was made for the attachment of a vacuum tube voltmeter. It was found that coarse adjustment could be made by varying the bias to V3. By adjustment of the battery tap supplies Ba1 and Ba2 the bias on tube V1 was made to lie between zero and three volts. Fine adjustment could then be made with the potentionmeter R40 controlling the bias to this tube.

The Dectector

Plate VI, Fig. 2 shows a photograph of the film holder. It was made from a 1/4 inch brass plate 3-1/2 inches wide by 11 inches long. Centered on it was a clamp which held the photographic film securely. The clamp was made from a 1/16 inch brass sheet 1-1/4 inch wide by 8 inches long with a 3/4 inch slot and was hinged to the film holder so that 35mm film 7-1/2 inches long could be inserted. A thumbscrew served to secure the clamp.

The film holder was fastened to the spectrograph by means of brass machine bolts with hexagonal heads. A crank with a hexagonal head socket attachment was used to facilitate quick removal of the film holder.

The Vacuum System

All parts of the system to which the ion beam had access were evacuated. The vacuum tightness of the instrument became the largest single problem of construction. In order to prevent seam splitting while soldering the pole faces, it was found necessary to silver-solder all brass joints. The large size of the instrument made it difficult to supply sufficient heat for even flow of the silver solder. This resulted in oxidation of many seams, with consequent leakage. To make these vacuum tight it was found necessary to chisel a V-groove in the faulty seams and fill with soft solder. As a final precaution all seams were covered with soft solder.

The system was evacuated by two diffusion pumps backed by the same Cenco Megavac fore-pump. The small defining slit at the source end effectively separated the evacuated region into two parts. For rapid pumping speed two pumps were thus employed.

Both diffusion pumps were manufactured by the Distillation Products Company. They were water-cooled and used a silicone oil pump fluid. A two-stage VMF, 10W pump evacuated the source end, while a three-stage, MCF 60 pump served to pump out the photographic plate section. All water connections were equipped with valves for the control of water-flow rate. The water and electrical connections are shown on Plate V. Plate VI, Fig. 3 is a photograph of the assembled instrument showing the placement of the two diffusion pumps. A desiccating flask, labeled C in Plate V, containing Dryite was inserted between the diffusion pumps and the fore-pump. This served to prevent contamination of the fore-pump

oil by water vapor. It was found necessary to separate the fore-pump from the wooden stand to prevent excessive vibration of the instrument. This was accomplished by attaching radio-mount shock pads on studs 5/8 inch in diameter by 6 inches long through the fore-pump anchor holes. The position of the fore-pump can be seen on Plate VI, Fig. 3.

The vacuum pressure down to 1 micron was measured by means of a thermocouple gauge. This proved convenient for observing whether the fore pressure was sufficiently low to start the diffusion pumps. A McLeod gauge was temporarily attached to measure pumping speed of the diffusion pumps. The McLeod gauge showed that a vacuum of 10^{-5} mm of mercury could be obtained in three hours and that a vacuum of 10^{-6} mm of mercury was attainable after twenty-four hours of pumping.

Provision for a Western Electric ion gauge, D79512, was made, as shown on Plates III, V and VI. The ion gauge control circuit is shown on Plate IX. The ammeter of this circuit was also used to measure the positive ion beam current from the tungsten filament source.

The regulation of the grid current of the ionization gauge was accomplished by means of two series connected transformers. If the grid current increased slightly the grid potential of the first 6V6 increased. This in turn, put a negative potential on the grids of the second and third 6V6's which caused a decreased current through the secondary of the transformer connected to the 6V6 plates. This increased the impedance of this transformer as seen from the primary side. Hence the current through this primary and the primary of the filament transformer was decreased.

EXPLANATION OF PLATE IX

Schematic Diagram of Ion Gauge Control

Values of Circuit Elements:

Tubes:
V1,V2 - 6SJ7
V3 - VR150
V4 - VR105
V5-V7 - 6V6
V8 - 83
V9 - 5Z3G

Choke:
L - 5mh 300ma

Transformers:
T1 - Thordarson T17R36
T2 - Stancor P8130
T3 - Sec. 700v 300ma
T4 - Sec. 5v 3 amp
T5 - Variac 200B
T6 - Sec. 768v,150ma,6.3v, 5 amp, 5v, 3 amp.

Capacitances:
C1, C2 - 0.1 microfarad
C3 - 0.001 microfarad
C4,C5 - 20 microfarads,450v.

Switches:
S1,S2 - DPST
S3 - 4P, 2 position

Meters:
M1 - 0-100 microamperes
M2 - 0-500 microamperes
M3 - 0-3 amperes AC
M4 - 0-300 volts
M5 - 0-10 milliamperes

Resistors:

R1	1K*	R13	25K*
R2	10K*	R14	15K*
R3	100K*	R15	220 ohms
R4	1 M***	R16	220 ohms
R5	47K*	R17	4.7K*3W**
R6	47K*	R18	2.2K*3W**
R7	1 M***	R19	1M***
R8	1 M***	R20	10K*
R9	4.7K*	R21	15K*3W**
R10	4.7K*	R22	10K*
R11	100 ohms	R23	100 ohms
R12	5.1K*1W**	R24	2 ohms

NOTE: *K = 1,000 ohms
**W = Watts
***M = 1,000,000 ohms

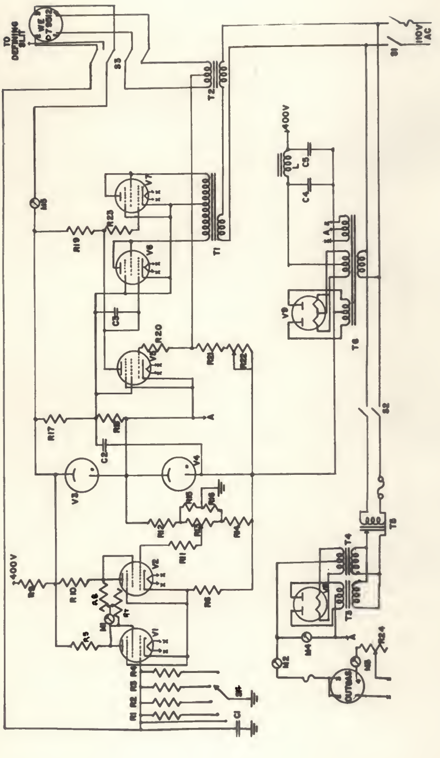

PLATE IX

This decreased the filament temperature and so returned the grid current to an equilibrium value. The positive ion current was measured on a vacuum tube bridge utilizing two 6SJ7 tubes. Four different grid resistors were available through switch S_4, which gave current sensitivities of 10^{-4} amp, 10^{-5} amp, 10^{-6} amp and 10^{-7} amp full scale. A plot of current versus bridge reading is shown on Plate X. Included in the ionization gauge control was a rectifier circuit which supplied current for outgassing the D79512 ion gauge tube.

EXPLANATION OF PLATE X

Graph of current versus current dial setting minus zero setting.

The following approximate current ranges are available:

Range 1 - Zero setting

Range 2 - Current reading times 10^{-4} amperes

Range 3 - Current reading times 10^{-5} amperes

Range 4 - Current reading times 10^{-6} amperes

Range 5 - Current reading times 10^{-7} amperes

PLATE X

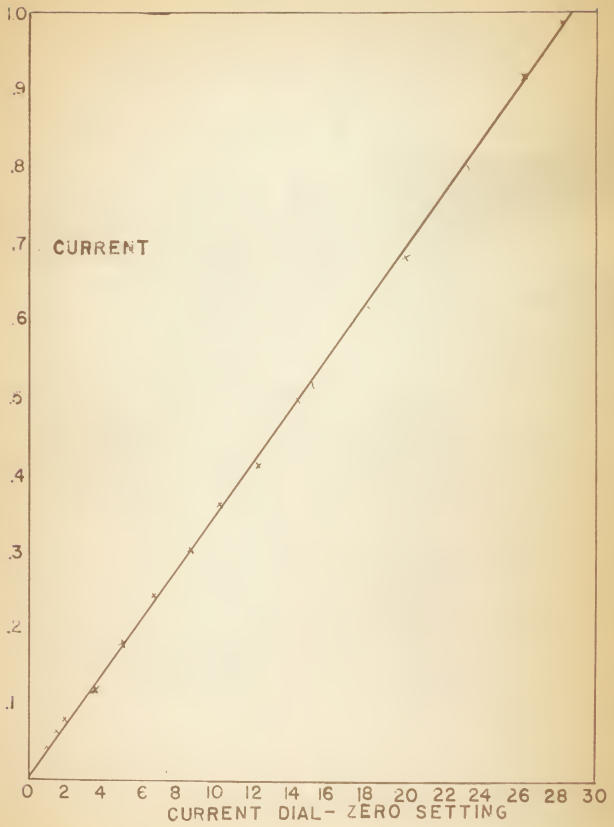
1.0
.9
.8
.7
CURRENT
.6
.5
.4
.3
.2
.1
0 2 4 6 8 10 12 14 16 18 20 22 24 26 28 30
CURRENT DIAL- ZERO SETTING

ACKNOWLEDGEMENTS

The author wishes to express his grateful appreciation to Dr. Clarence M. Fowler for the interest, the advice, the encouragement, and the help extended by him throughout the course of this research; to Dr. Louis D. Ellsworth for his frequent advice and assistance on the electronics apparatus; to Dr. Robert M. McFarland for his advice and assistance on vacuum problems; to Dr. R. Dean Dragsdorf for his help with the construction of the ion gauge control unit; to Mr. Roy C. More for the precision grinding of the pyrex glass spacers; to Mr. Duane A. Rittis for his indispensable advice and help on many construction details; to Professor Emeritus Eustace V. Floyd for his willing advice on construction details; and to the Atomic Energy Commission for their sponsorship of the author's half-time Assistantship throughout most of this work.

LITERATURE CITED

(1) Bainbridge, Kenneth T. and Jordan, Edward B.
Mass Spectrum Analysis. Phys. Rev. 50: 282. 1936.

(2) Blewett, J. P. and Jones, E. J.
Filament Sources of Positive Ions. Phys. Rev. 50: 464. 1936.

(3) Kerwin, Larkin and Geoffrian, Claude.
Magnetic Focussing. Rev. Sci. Inst. 20:36. 1949.

(4) Lewis, Lloyd G. and Hayden, Richard J.
A Mass Spectrograph for Radioactive Isotopes. Rev. Sci. Inst. 19: 599, Erratum 922. 1949.

(5) Mattuch, Josef.
A Double-Focussing Mass Spectrograph and the Masses of N^{15} and O^{18}. Phys. Rev. 50: 617. 1936.

(6) Nier, A. O.
A Mass Spectrometer for Isotope and Gas Analysis. Rev. Sci. Inst., 18: 398. 1947.

(7) Thomson, J. J.
Cathode Rays. Phil. Mag. and J. of Sci., Fifth Series, 505: 293. 1897.

(8) Thomson, J.J.
Rays of Positive Electricity. Phi. Mag. and J. of Sci., Sixth Series 20: 752. 1910.

THE DESIGN AND CONSTRUCTION OF A MASS SPECTROGRAPH

by

KEITH A. MORE

B. S., Kansas State College of Agriculture and Applied Science, 1951.

AN ABSTRACT OF A THESIS

Submitted in partial fulfillment of the

requirements for the degree

MASTER OF SCIENCE

Department of Physics

KANSAS STATE COLLEGE

OF AGRICULTURE AND APPLIED SCIENCE

1953

A mass spectrograph is an instrument which is capable of separating isotopes according to their mass. The operation depends on the fact that a moving charged particle has a circular path in a magnetic field where the radius of curvature is given by

$$R = K\sqrt{M} \qquad K = \frac{10\sqrt{2E}}{Be}$$

E is the kinetic energy in ergs, B is the magnetic field in gauss and e is the charge of the electron in coulombs.

The mass spectrograph that was designed and constructed was to be used for analyzing a sample in order to ascertain the isotopes that it contained and also was to be used as a small-quantity separator in the rare-earth region.

The design was of the '60 degree sector' type with a radius of curvature of 14 cm for the symmetrically focussed ion beam. It consisted of an ion source using positive ion emission from a hot filament. A magnetic field defined by hexagonal pole pieces giving '60 degree type focussing' and a photographic plate detector.

The ion beam was accelerated by a high potential obtained from a well regulated scaling circuit supply. This potential was placed between a tungsten filament and a nichrome disc which were separated by 1 cm. The nichrome disc had a collimating slit and was connected through an ammeter to the ground of the high voltage unit. The ammeter measured the ion current which was collected by the collimating disc. This current was taken as proportional to the ion beam current.

The magnet was made of Armco iron. Two coils, each of 12,000 turns of 24 B&S gauge, Formvar-coated, copper wire were used in series.

A field of 5,000 gauss was obtained with a current of 150 milliamperes. The magnet current was well regulated up to 500 milliamperes by comparing the voltage drop across a manganin resistor connected in series with the coils. Any variation in the voltage across the resistor was automatically adjusted by an electronic circuit so that the current was held constant.

The photographic plate detector lay in a plane which passed through the center of curvature of the symmetrically focussed ion beam and the source.

The system was evacuated by two water-cooled, oil diffusion pumps, one a two-stage pump at the source end, the other a three-stage pump for the photographic plate section. Both pumps were backed by the same Cenco Megavac mechanical fore-pump. The fore-pump vacuum pressure was measured by a thermocouple gauge. Provision was made for a Western Electric D79512 ion gauge tube for high vacuum measurements.